

Evaluation of Tumor Growth in Treatment of Murine Melanoma by Transdermal Infusion of Etoposide by Radiofrequency

Salomao-Junior A^{1,2}, D'Agostino LG^{1,2}, Luna ACL^{1,2}, Menezes FC^{2,3}, Viana DC⁴, Rodrigues CJ⁵ and Maria DA^{1,2*}

¹Biochemistry and Biophysics Laboratory, Butantan Institute, Sao Paulo, Brazil

²Faculty of Medicine, Medical School, University of Sao Paulo, Sao Paulo, Brazil

³Department of Dermatology, Faculty of Medicine, University of São Paulo, São Paulo, Brazil

⁴Department of Surgery, Faculty of Veterinary Medicine and Animal Science, University of Sao Paulo, Sao Paulo, Brazil

⁵Department of Orthopedics and Traumatology, Faculty of Medicine, University of Sao Paulo, Sao Paulo, Brazil

*Corresponding author: Durvanei Augusto Maria, Faculty of Medicine, Medical School, University of Sao Paulo, Sao Paulo, Brazil, Tel: 55-11-2627-9750; Email: durvanei@usp.br

Received date: November 23, 2015; Accepted date: January 18, 2016; Published date: January 22, 2016

Copyright: © 2015 Salomao-Junior, et al. This is an open-access article distributed under the terms of the Creative Commons Attribution License, which permits unrestricted use, distribution, and reproduction in any medium, provided the original author and source are credited.

Abstract

Objective: In order to make such a substance cross the epidermal barrier, was utilized a method of transdermal drug delivery system (TDDS) combined with the chemotherapeutic etoposide in the treatment of dorsal melanoma B16F10 tumor on C57BL/6J mice.

Methods: The treatment groups were as follows: etoposide followed by radiofrequency (RF); RF followed by etoposide; etoposide and controls. The animals were treated with delivery interval of 72 hours, for 20 days and were analyzed the tumor growth; weight and hematological profile. The histological analysis and cell cycle by flow cytometry were performed after end of the treatment period.

Results: The tumors treated with RF followed by etoposide showed slower growth compared to the tumors treated with etoposide followed by RF, and found that treatment with radiofrequency considerably increased the dorsal tumor growth. In fact, the increase in tumor mass is because the radiofrequency cause an inflammatory response and stimulate collagen production by fibroblasts.

Conclusions: The results showed that the treatment groups RF followed by etoposide showed a high rate sub-G1 phase cells, indicating better therapeutic efficacy. Therefore, it is important to clarify that the referred technologies are not as harmless as it has been reported.

Keywords: Melanoma; Etoposide; Cancer chemotherapeutic; Collagen stimulation; Skin permeation, Radiofrequency; Transdermal drug delivery system

Introduction

The incidence of melanoma cases is increasing worldwide and despite early detection, appropriate surgical resection and adjuvant therapy, the number of patients dying from metastatic disease continues to rise. According to the World Health Organization, approximately 80% of all skin cancer-related deaths are attributed to melanoma, although it comprises only 5% of all skin cancers [1]. The prognosis of advanced melanoma remains poor, with the median survival ranging from 6 to 9 months with chemotherapy [2,3]. Survival outcomes for patients with advanced disease vary depending on the number of adverse prognostic factors that are present such as visceral disease or brain metastases and whether or not serum lactate dehydrogenase levels are elevated [3-6]. Despite extensive clinical research, the treatment options for metastatic disease were limited, with melanoma being considered as one of the most chemotherapy-resistant. Many agents have been investigated in terms of their antitumor activity in melanoma, but the efficacy of treatment remained poor [3,7].

Numerous cytotoxic agents, as single agents and in combinations, have been evaluated for the treatment of metastatic melanoma but none has ever demonstrated a survival advantage. Nevertheless, several chemotherapy regimens are often used in advanced disease, including dacarbazine (DTIC) and temozolomide. DTIC is the only chemotherapeutic agent approved by the Food and Drug Administration for treatment of melanoma and is often considered "standard" therapy for advanced melanoma, despite its limited activity. DTIC is considered the most active single agent in patients with melanoma; however, relative response are <20%, complete responses are rare, and a survival advantage has never been demonstrated [8].

Etoposide is a semi-synthetic derivative of podophyllotoxin poorly soluble in water [9]. At low concentrations, this drug inhibits the entry of neoplastic cells in prophase, probably due to its action on topoisomerase II [9]. At high concentrations, the lysis of cells entering mitosis is observed. The predominant molecular effect is the inhibition of DNA synthesis. The cytotoxicity and apoptosis induced by etoposide were studied for 72 hours in human melanoma cells. Etoposide initially damages DNA by ATM kinase and by activating p53 and caspase 2 pathways. Consequently, there is an initial increase in the amount and activity of mitochondria of target cells, but which are subsequently suppressed. These changes were not preceded by loss in membrane

potential and the release of cytochrome c. After oral administration, distribution in cerebrospinal fluid is variable and weak; etoposide is mostly distributed in the liver, kidneys, brain, heart and intestines [9].

The transdermal drug delivery system (TDDS) is used, due the low efficacy of the traditional chemotherapy used in the treatment of melanoma and many side effects. TDDS has been recognized as a promising route for administration of drugs used in the treatment of local and systemic diseases [10-15]. TDDS has many advantages compared to oral administration. The main advantage is the non-occurrence of the effects observed when the drug crosses the liver for the first time and a significant amount of the drug is metabolized too fast [15,16]. One limitation of this technique is that only a reduced number of drugs can be administered by this route. Only low molecular weight drugs can be used (a few hundred Daltons). This is the main difficulty of the infusion of hydrophilic drugs, macromolecules and peptides. TDDS by thermal ablation through fractionated radiofrequency device is a method that permeates the skin by means of columns of coagulation in the epidermis and dermis generated by the fractionated heat source. This technology concentrates RF energy in small electrodes. They do not have subcutaneous action without side effects damage [15,17].

This paper used TDDS by thermal ablation combined with the chemotherapeutic agent etoposide in the treatment of dorsal tumor on mice bearing melanoma. We evaluated to utilize etoposide because it is a liposoluble drug and the aim of this paper was to study the passage of substances with such characteristics through the epidermis. In order to make such a substance cross the epidermal barrier, was utilized the method of transdermal drug delivery system (TDDS).

Materials and methods

Animals

Twenty five isogenic C57BL/6J female mice weighing 26 ± 2 g and about 2-4weeks old, supplied by Animal Laboratory of the Butantan Institute (São Paulo, Brazil), were used in the experiment. The animals were housed in a temperature-controlled room at 25 °C, with food and water provided ad libitum. All experimental procedures were carried out in accordance with the guidelines for animal experimentation determined by the Canadian Council Animal Care. The study protocol was approved by the Institutional Animal Care from Butantan Institute (process number 927/12).

Melanoma tumor cells implantation in mice

The B16F10 (CRL-6475) melanoma cell line was obtained from American Type Culture Collection (ATCC, Manassas, VA). The melanoma cell line was cultured in RPMI-1640 (Sigma, St. Louis, MO) supplemented with 10% heat-inactivated fetal calf serum (Cultilab, Campinas, Brazil), 2 mM L-glutamine (Gibco, Carlsbad, United States), 5 mM 2-mercaptoethanol (Gibco, Carlsbad, United States), penicillin and streptomycin (100 µg/mL; Gibco, Carlsbad, United States). Cells were incubated at 37 °C in a humidified incubator containing 5% CO₂. The mice were shaved on the dorsal surface and weighed. Subsequently, with the aid of a sterile syringe 106/tumor cells were inoculated subcutaneously in the dorsal area of the mice.

To evaluate the time of the melanoma cell growth in mice was determined after the subcutaneous (sc) inoculation of melanoma cells.

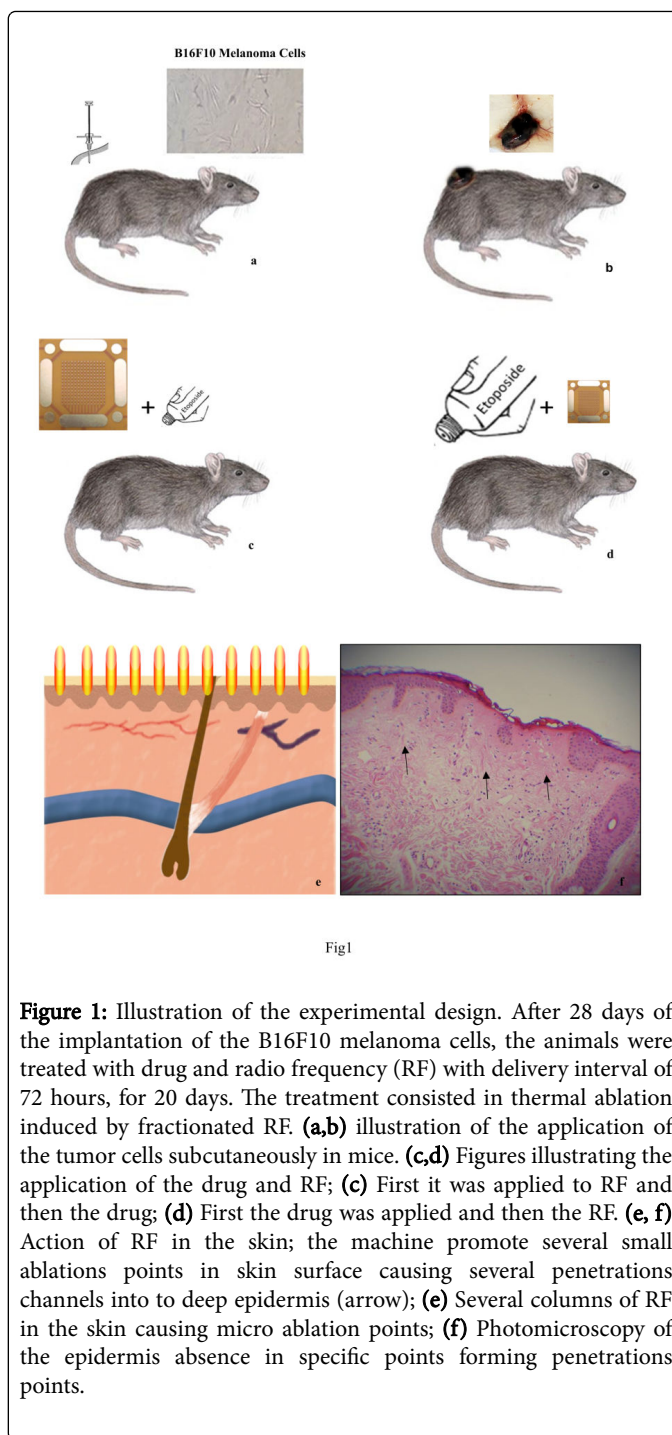


Fig 1

Figure 1: Illustration of the experimental design. After 28 days of the implantation of the B16F10 melanoma cells, the animals were treated with drug and radio frequency (RF) with delivery interval of 72 hours, for 20 days. The treatment consisted in thermal ablation induced by fractionated RF. (a,b) illustration of the application of the tumor cells subcutaneously in mice. (c,d) Figures illustrating the application of the drug and RF; (c) First it was applied to RF and then the drug; (d) First the drug was applied and then the RF. (e, f) Action of RF in the skin; the machine promote several small ablations points in skin surface causing several penetrations channels into to deep epidermis (arrow); (e) Several columns of RF in the skin causing micro ablation points; (f) Photomicroscopy of the epidermis absence in specific points forming penetrations points.

Evaluation of tumor growth

During the experimental period, tumor growth and animal weight were evaluated. The assessment of tumor growth was performed on a weekly basis by measuring the dimensions of length and width of the tumor masses with a digital caliper (Mitutoyo, measurement 0.01 mm), the tumor volume was calculated using the formula: length × (width)²/0.52. Tumor growth was photographic documentation with a digital camera (Model Sony).

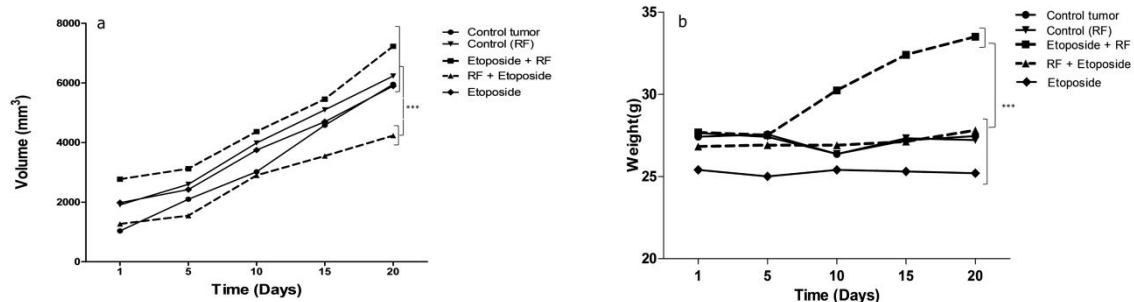


Fig2

Figure 2: Determination of tumor volume and weight of C57BL/6 mice bearing B16/F10 melanoma. Results represent means from three independent experiments. The standard deviation has not been shown in the graphs to facilitate comparisons between values obtained to the concentrations used during the days analyzed. During the treatment duration (20 days), tumor growth and animal weight were evaluated in the different experimental groups. **(a)** Tumor volume (mm³). **(b)** Weight of the animals. Statistical differences ***p<0.001.

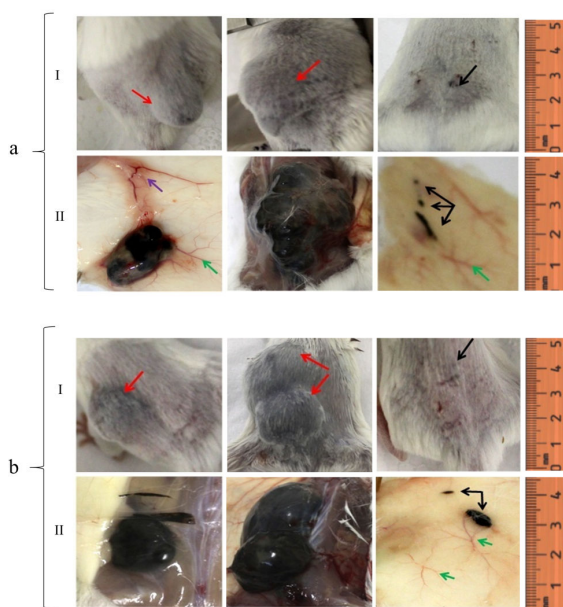


Fig3

Figure 3: Macroscopic aspects of C57BL/6 mice bearing B16/F10 melanoma, after 20 days of treatment. Results represent means from three independent experiments. After the end of the treatment cycle, the animals were euthanized and the abdominal cavity and internal organs were macroscopically observed. Animals treated with **(a)** RF followed by etoposide. **(b)** Etoposide followed by RF. **(I)** Pre- euthanasia; **(II)** Post- euthanasia.

Treatment of the animals with melanoma

After 28 days of the implantation of the tumor cells, mice were randomly distributed into 5 experimental groups to observe the

therapeutic effect of the different treatment strategies. The treatment groups were as follows:

Etoposide + RF: mice with tumor treated with etoposide followed by RF (n=05).

RF + etoposide: mice with tumor treated with RF followed by etoposide (n=05).

Etoposide: mice with tumor treated with etoposide only (n=05).

Control RF: mice without tumor treated with RF + etoposide (n=05).

Control tumor: mice with tumor without treatment (n=05).

The animals were treated with delivery interval of 72 hours, for 20 days, totalling seven applications. The treatment consisted in thermal ablation induced by fractionated RF. A thin layer of the chemotherapy (etoposide) was applied on the animal's skin surface without friction immediately before and after radiation, according to the proposed treatment group, which has a concentration of 34 mM of etoposide [18]. The equipment used was Eunsung, Duet RF model, which is heated with bipolar radiofrequency electrodes.

The device supplies 300W power has resistance-type radiofrequency and various densities. The spot used has a density of 100 points/cm². Spots are of metal material to allow electrons to flow freely. The amount of heat energy used was 39 joules, duration of the pulse was 0.4s, level II on the dorsal area in a single session (Figure 1).

Analysis of hematological profile

The hematological profile of mice in the different treatment groups was determined on the 1th, 10th, 15th and 20th days after initiation of treatment. Approximately 20 µl of blood was collected from mice retro-orbital sinuses with heparinized capillary tubes. White blood cells, red blood cells and platelets were manually counted using a Neubauer hemocytometer chamber and the differential white blood cell count was performed by smear blood to count of the leukocytes types.

Necropsy of animals

After the end of the treatment cycle, the animals were euthanized with the use of anesthetics (ketamine hydrochloride 35 mg/kg and hydrochloride xylazine 80 mg/kg) followed by cervical dislocation and then necropsied. Macroscopic analysis of the tumor followed by sampling of tumor masses and irradiated adjacent tissue were performed. The collected tumor masses were macerated in digestion solution with 0.2 U/ml of collagenase type IV (Gibco, Carlsbad, United States), filtered and stored in 70% alcohol for determination of the cell cycle. Samples of tumors were stored at -20 °C until analysis.

The abdominal cavity and internal organs (heart, lungs, liver, kidneys, lymph nodes, spleen, brain and Peyer's plaques) were macroscopically observed in the search for possible metastases. Then, the internal organs were weighed and placed in buffered formalin for subsequent histopathological analysis.

Cell cycle phase analysis by flow cytometry

After digestion collagenase, 106 tumor cells were incubated at 37 °C for 45 min in 0.5 mL PBS and then stained with propidium iodide (PI) for 30 min at 37 °C. The cells were centrifuged, and the pellets were resuspended with 5 mL of cold 70% ethanol and fixed overnight at 4 °C. The fixed cells were washed twice in PBS and incubated with RNase (100 g/mL) and PI (50 µg/mL) at room temperature in dark. Flow cytometric analysis was performed with a FACScalibur (Becton Dickinson, San Jose, CA, United States). Data from a minimum of 10,000 cells were collected and analyzed with CellQuest software. The DNA content in the cell cycle phases (sub-G1, G0/G1, S and G2/M) was analyzed by ModFit LT 3.2 software (Becton Dickinson, San Jose, CA, United States).

Histopathological analysis of tumors

The specimens were sent to the routine histological processing, following the standard protocol. Histological sections (5 µm) from all organs removed were stained with hematoxylin and eosin (HE) and examined by Olympus VS110 system that allows to combine microscopy to image.

The following parameters were examined in the samples of B16F10 murine melanoma tumors: 1) size; 2) symmetry; 3) restraint systems; 4) maturation; 5) pagetoid spread; 6) necrosis/ulceration; 7) inflammatory infiltrate; 8) regression; 9) cellular atypias; 10) mitosis; 11) melanization; 12) isolated cells proliferation. Histological sections were analyzed by a pathologist in a blind procedure.

Statistical analysis

The ANOVA variance test was used to compare the results of blood cell counting, tumor growth and cell cycle distribution. The Tukey' Test was used to compare the number of animals with metastatic nodes in the studied groups. The graphics were obtained by Prism version 5.0. All the values were expressed as means ± S.D. from three independent and statistical significance (p-value) *p < 0.05, **p < 0.01 and ***p < 0.001.

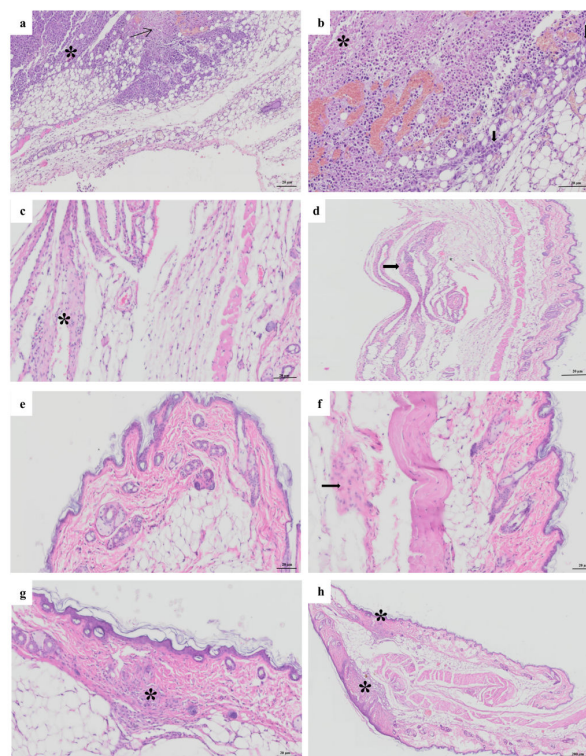


Fig4

Figure 4: Photomicroscopy of the subcutaneous tissue of C57BL/6 mice bearing B16/F10 melanoma, after 20 days of treatment. After the end of the treatment period, the animals were euthanized and the organs were collected for histological analysis. **(a, b)** Control tumor group; **(a)** Showing marked subcutaneous tissue by tumor infiltrating mononuclear cells (*). Note the presence of areas of necrosis (arrow); **(b)** Subcutaneous tissue showing invasion by tumor cells (melanocytes). These cells show on apoptosis and necrosis. With the presence of nuclear pyknosis. Presence of coagulation necrosis area (*). Note small area on the deepest portion showing preserved tumor cells (arrows). **(c,d)** Group treated with Etoposide; **(c)** Subcutaneous tissue showing healing process (increase of fibroblasts and collagen and presence of mononuclear cell infiltration (*)); **(d)** Showing areas of skin healing process encompassing dermis and subcutaneous tissue (*). **(e,f)** RF followed by etoposide; **(e)** Skin showing the epidermis, dermis and skin appendages without histological changes; **(f)** Skin showing the epidermis, dermis, skin appendages without histological changes. Note area subcutaneous tissue showing healing process (increase of fibroblasts and collagen - arrow). **(g,h)** Etoposide followed by RF; **(g)** Showing skin healing process area with increasing fibroblast, collagen and mononuclear inflammatory cells (*); **(h)** Skin showing the epidermis, dermis and subcutaneous tissue attachments without histological changes.

Result

Tumor volume and animal weight

During the experimental period, tumor growth and animal weight were evaluated in the dorsal area of the mice by measuring the volume and body weight gain. After the experiment was observed that occurred the tumor growth, so at 20 days after therapy the tumor mass was $5956 \pm 8.3 \text{ mm}^3$ for the control tumor group; $6232 \pm 9.3 \text{ mm}^3$ for control (RF) group; $7231 \pm 10 \text{ mm}^3$ for the etoposide followed by RF group (ER); $4232 \pm 7.6 \text{ mm}^3$ for the RF followed by etoposide group (RE) and $5898 \pm 6.0 \text{ mm}^3$ for the RF group (Figure 2 a). The tumors treated with RE showed slower growth compared to the tumors treated with ER and all other treatment groups (** $p < 0.001$).

The final weight of the animals treated with RE were lower than those of the animals treated with ER, with average values of weight of $27.8 \pm 1.0\text{g}$ and $33.5 \pm 1.1\text{g}$, respectively (** $p < 0.001$). The weight of

the animals of the other treatment groups was $27.2 \pm 1.1\text{g}$ for RF; $25.2 \pm 1.0\text{g}$ for etoposide group and $27.5 \pm 1.0\text{g}$ for the control tumor group. All groups showed significant differences with ER (** $p < 0.001$) (Figure 2 b).

Macroscopic aspect of the melanoma tumor

Forty-eight days after tumor cell inoculation the animals developed nodular and flat, pigmented and non-ulcerative tumors in the dorsal area in the treatment groups that showed tumor growth. In both treatment groups, the tumors were nodular in the dorsal area, with a great variation between them (large, small and radial). Intense vascularization was observed in peripheral areas next to the tumor mass, in the subcutaneous tissue. The animals with tumors did not show signs of cachexia (Figure 3).

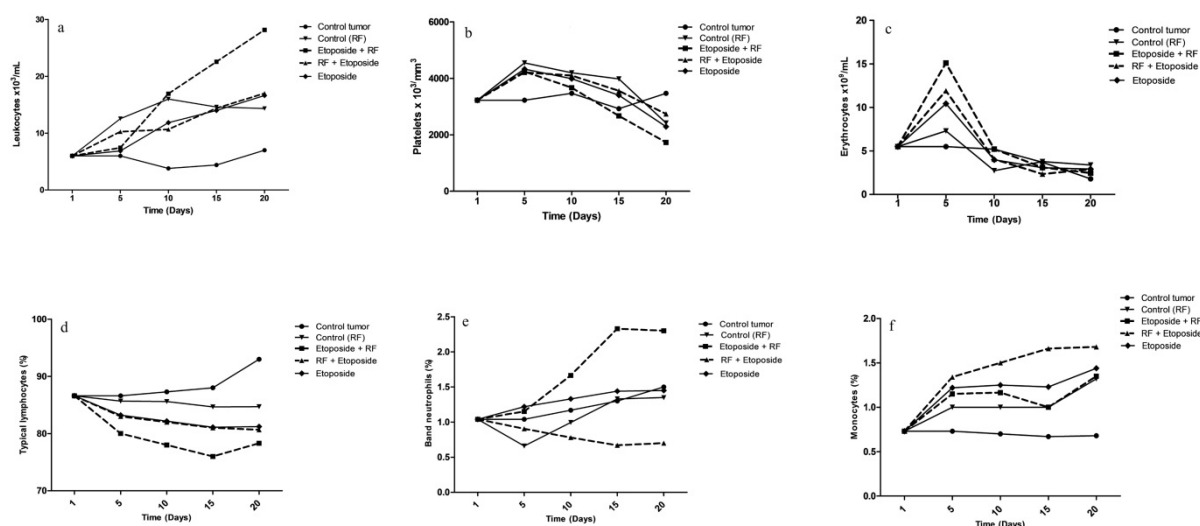


Fig5

Figure 5: Hematological parameters and differential count of C57BL/6 mice bearing B16/F10 melanoma, after 20 days of treatment. Results represent means from three independent experiments. The standard deviation has not been shown in the graphs to facilitate comparisons between values obtained to the concentrations used during the days analyzed. (a) Leukocytes. (b) Platelets. (c) Erythrocytes. (d) Typical lymphocytes. (e) Rod – shaped segmented neutrophils. (f) Monocytes.

Histopathology analysis

The control tumor group showed subcutaneous tissue showing invasion by tumor cells with the presence of nuclear pyknosis and cariorex. The nucleus to cytoplasm ratio very disproportionate. Presence of necrosis, bleeding and lymphocytes with extensive areas of melanin pigments (Figure 4a and 4b). The group treated with etoposide showed the epidermis, dermis, and subcutaneous tissue attachments without histological changes (Figure 4c and 4d). The tumor group treated with RF+etoposide presented tumor area with neoplasia of pigmented cells forming blocks with necrotic areas. The pyknotic cells and other with melanocytic cells were showed in peripheral area. Skin showing the epidermis, dermis and skin appendages without histological changes. Subcutaneous tissue showing healing process with of fibroblasts and collagen deposition (Figure 4e and 4f).

The tumor group treated with etoposide + RF showed subcutaneous tissue showing healing process increase of fibroblasts and collagen and presence of mononuclear cell infiltration. Showing skin healing process areas encompassing dermis and subcutaneous tissue. Area with marked cellular atypia. Accumulation of fusiform and rhomboidal cells (Figure 4g and 4h).

Hematological profile

The evaluation of the progressive increase haematological profile of mice with melanoma tumor inoculated in the dorsal area was performed after collection of 5 samples of peripheral blood, before and after starting the treatment.

The number of leukocytes increased significantly, 20 days after the start of treatment. So the largest increase was observed in etoposide + RF group, significantly different from all other groups, with values of $28.2 \pm 2.1 \times 10^3/\text{ml}$. The average number of leukocytes to other groups

were $7.0 \pm 1.2 \times 10^3/\text{ml}$ for the control tumor group; $14.3 \pm 1.4 \times 10^3/\text{ml}$ control (RF) group; $16.6 \pm 0.9 \times 10^3/\text{ml}$ for etoposide group and $17.0 \pm 1.2 \times 10^3/\text{ml}$ for RF + etoposide (Figure 5 a). A significant decrease in platelet counts was observed among all treatment group, 20 days after the start of treatment, in relation to the tumor control group, with average number of $3469 \pm 5.4 \times 10^3/\text{mm}^3$ (control tumor group); $2740 \pm 2.7 \times 10^3/\text{mm}^3$ (RF + etoposide); $2420 \pm 2.6 \times 10^3/\text{mm}^3$ (control RF group); $2291 \pm 3.1 \times 10^3/\text{mm}^3$ (etoposide) and $1730 \pm 2.3 \times 10^3/\text{mm}^3$ (etoposide + RF). There were significant differences among the etoposide + RF and all other groups (Figure 5b).

The percentage of erythrocytes increased significantly, 5 days after the start of treatment, in the etoposide group ($10.4 \pm 1.3 \times 10^9/\text{ml}$), RF + etoposide ($11.9 \pm 1.5 \times 10^9/\text{ml}$) and etoposide + RF ($15.1 \pm 1.0 \times 10^9/\text{ml}$), in relation to the tumor control group ($5.5 \pm 0.5 \times 10^9/\text{ml}$). However, after 20 days, there was a significant percentual decrease in the percentage of erythrocytes, among the experimental groups

($***p < 0.001$), there were no differences among them (Figure 5 c). The percentage of typical lymphocytes increased significantly ($**p < 0.01$) in the tumor control group, 20 days after the start of treatment, with values of $93 \pm 2.3\%$. However, it was observed a significant decrease of typical lymphocytes in the treatment groups, in relation to the tumor control group ($***p < 0.001$), with average number of $80.7 \pm 0.5\%$ for RF + etoposide and $78.3 \pm 0.8\%$ for etoposide + RF, in principle, the difference is statistically significant ($*p < 0.05$) (Figure 5 d). The number of band neutrophils decreased significantly in the RF + etoposide group ($**p < 0.01$), after 20 days, with value of $0.7 \pm 0.2\%$, compared with the tumor control group ($1.5 \pm 0.3\%$). However, in the etoposide + RF group, there was significant increased, with value of $2.3 \pm 0.8\%$ ($**p < 0.01$) (Figure 5e). After the treatment, it was observed a significant increase in the number of monocytes, among all treatment and control group (RF), compared with tumor control group ($***p < 0.001$) (Figure 5f).

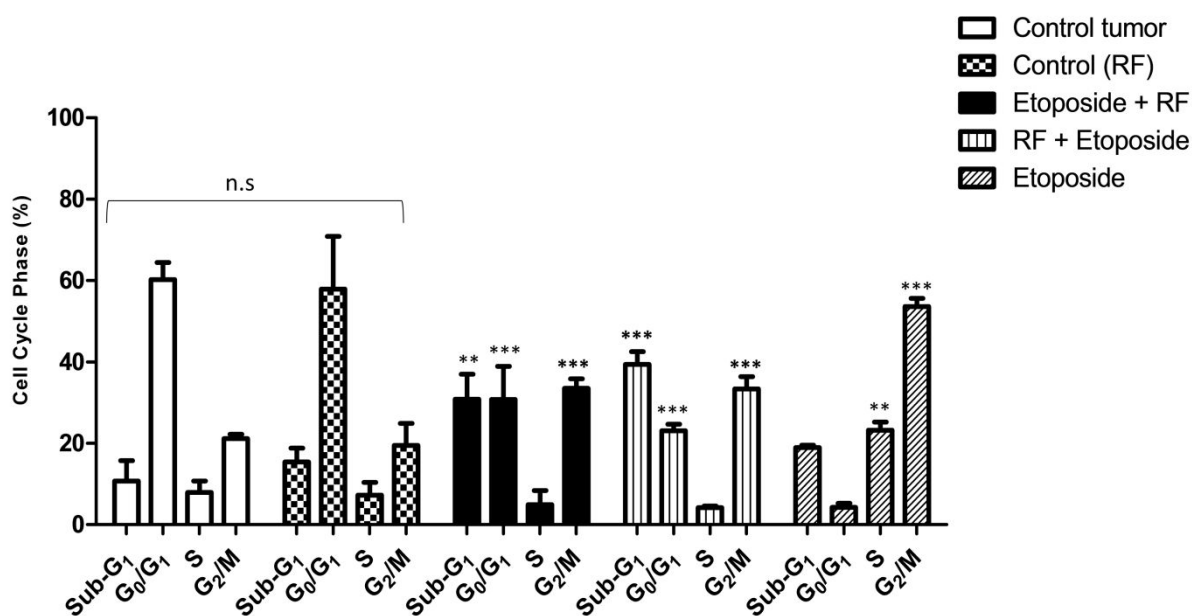


Fig6

Figure 6: Analysis of cell cycle phases of tumor cells treated. Results represent means \pm S.D. from three independent experiments, obtained by flow cytometry analysis. Proportion of tumor cells residing in sub-diploid; G0/G1; S and G2/M phases. Statistical differences $*p < 0.05$; n.s.=no significance.

Cell cycle phases distribution

Cell cycle phases distribution was performed from fractions of the tumor, collected after the end of the treatment period. The cell cycle analysis results are shown in figure 6. There were no significant differences in cell cycle parameters between tumor control group and control (RF). The results demonstrate that the treatment groups etoposide + RF and RF + etoposide, showed significant increase of sub-G1, compared to tumor control group ($10.7 \pm 5.0\%$), with values of $30.8 \pm 6.2\%$ and $39.4 \pm 3.1\%$, respectively. Cells rates in G0/G1 phase of the cell cycle were high in both tumor control and control group treated only by radiofrequency. Indicating a high rate of cell activity. However, There was an increase in the G0/G1 phase cells in all

treatment, compared to control groups ($60.2 \pm 4.1\%$ for tumor control group and $57.9 \pm 12.9\%$ for control RF), with values of $30.8 \pm 8.1\%$ (etoposide + RF); $23.1 \pm 1.6\%$ (RF + etoposide) and 4.3 ± 1.0 (etoposide). The only statistically significant difference is among etoposide group ($23.1 \pm 2.0\%$), tumor control group ($7.9 \pm 2.8\%$) and control RF ($7.2 \pm 3.1\%$). The percentage of cells in G2/M was greater among treatment groups etoposide + RF ($33.5 \pm 2.3\%$), RF + etoposide ($33.3 \pm 3.3\%$) and etoposide ($53.6 \pm 2.0\%$). Obtaining statistical difference compared to tumor control groups ($21.1 \pm 1.1\%$) and control RF ($19.5 \pm 5.4\%$). The cytometry results of etoposide group showed greater phase cells rate S and G2/M, apparently acting in pre-mitotic phase of cell division to inhibit DNA synthesis; is dependent

upon the particular cell cycle phase and with a maximum effect on the S and G2 phases of the cell division (Figure 6).

Discussion

Due to the recent advances in technology and the incorporation of the drug to the site of action without rupturing the skin membrane transdermal route is becoming the most widely accepted route of drug administration. It promises to eliminate needles for administration of a wide variety of drugs in the future. TDDS have great potentials, being able to use for both hydrophobic and hydrophilic active substance into promising deliverable drugs [13].

TDDS have many advantages over other conventional dosage forms and these are reduced side effects, sustained drug delivery, removal of first-pass metabolism [19-22]. For effective TDDS, drug should enter beneath the skin to reach the targeted place [23,24]. One way to create these thermal ablation microchannels in the skin is by using radiofrequency waves [25]. These waves cause ions in the surrounding cells to vibrate, the vibrations cause heat, the heat causes evaporation, and the evaporation of water from the cells causes ablation. The radiofrequency involves the exposure of skin to high frequency alternating current (~100 kHz) which produces microscopic passages in the stratum corneum [26]. As performances proof it has demonstrated in vivo studies that plasma level of granisetron hydrochloride (serotonin 5-HT₃ receptor antagonist) after 12 hours was 30 times greater when previously exposed to radiofrequency than the level recorded for untreated skin after 24 hours [26]. In the same research was demonstrated similar effect of permeability of diclofenac sodium through the skin [26]. The drug delivery rate is influenced by the number and depth of these microchannels produced [26]. The present study showed that, besides the TDDS has increased drug penetration in the skin, there are significant differences in the results between sequences of application of etoposide in the skin mice. In the mice group treated first with the drug and after with RF, the tumor growth was significantly greater. This can be an indicative that the aggression suffered by the tumor by RF stimulates the growth [18]. It could be an evidence that when the drug is applied before RF, it is destroyed by heat generated by the technology. In fact the RF system heats the skin up to temperatures about 70-80 °C [27]. According previous studies, the RF system can stimulate the collagen production by local aggression of the dermal tissue [28,29]. In this way, if it stimulates fibroblasts by local aggression, could it stimulates a tumor growth? Could a RF device stimulate a dysplastic nevus to become a tumor? In fact, the increase in tumor mass is because the radiofrequency cause an inflammatory response and stimulate collagen production by fibroblasts, confirming the histopathological findings and results obtained by analysis of the cell cycle by flow cytometry [28,29]. Therefore, it is important to clarify that the referred technologies are not as harmless as it has been reported. New studies and experiments must be done to elucidate comprehensively all mechanisms involved in effects of RF in human tissues.

The evaluation of the phase distribution of cells throughout the cycle has been carried out by incorporation of propidium iodide, a fluorochrome which intersperses stoichiometrically every four base pairs of DNA [30]. The results were expressed as mean percentage of cells in different cell cycle phases. Fragmented DNA, quiescent phase G0/G1, phase synthesis - S and G2/M. The results showed that the treatment groups RF + etoposide showed a high rate sub-G1 phase cells, indicating better therapeutic efficacy. Obtaining statistical difference compared to others groups. Cells rates in G0/G1 phase of

the cell cycle were high in both tumor control and control group RF. Demonstrating the potential stimulatory effect of tumor growth.

On the other hand, in the mice group treated first with RF and then the drug, there were lower rates of tumor growth. With the permeability optimized the drug produces the desired therapeutic effect, that is, decrease tumor growth. These data suggest that treatment with RF followed by application of the chemotherapeutic agent was more effective in controlling the growth of B16F10 melanoma. From the haematological point of view, the sequence of etoposide followed RF increased depletion of lymphocytes. The sequence of RF followed etoposide noted a decrease in tumor growth and less myelosuppression. Could this local chemotherapy be an alternative for tumors that cannot be surgically resected due metastases or satellites lymph nodes? Or could be a new alternative therapy for immunosuppressed patients? This therapeutic approach would have less immunosuppressive effects while maintaining therapeutic response? Could be an adjunct to surgical treatment? Could it have a synergistic effects with other techniques, such as chemotherapy embolization? The TDDS maybe an alternative treatment for cutaneous metastases from non-melanoma tumors with chemotherapy resistance and an alternative to radio-resistant melanoma.

The choice of the method, as well the sequence of application plays a key role in the expected clinical outcomes. Therefore, it is concluded that if there is a correct sequence of transdermal drug delivery system application, it would be as follows: first radiofrequency and after the drug administration (in our case etoposide). The opposite sequence increased the tumor growth rate. In other words, there was a significant increase in tumor size after application of etoposide followed RF. In fact, the RF system can stimulate the collagen production by local aggression of the dermal tissue. The RF cause an inflammatory response, confirming the histopathological findings and results obtained by analysis of the cell cycle by flow cytometry. New studies and experiments must be done to elucidate comprehensively all mechanisms involved in effects of RF, in this case.

Therefore, it is important to clarify that the referred technologies are not as harmless as it has been reported. New studies and experiments must be done to elucidate comprehensively all mechanisms involved in effects of RF in human tissues.

On the other hand, in group treated first with RF and then the drug, there were lower rates of tumor growth. With the permeability optimized the drug produces the desired therapeutic effect, that is, decrease tumor growth. It worked like a local chemotherapy without systemic effects. It deserves be better studied due the several new clinical indications that could have.

References

1. World Health Organization (2012) Skin cancers.
2. Garbe C, Eigentler TK, Keilholz U, Hauschild A, Kirkwood JM (2011) Systematic review of medical treatment in melanoma: current status and future prospects. *Oncologist* 16: 5-24.
3. Coventry BJ, Baume D, Lilly C (2015) Long-term survival in advanced melanoma patients using repeated therapies: successive immunomodulation improving the odds? *Cancer Manag Res* 7: 93-103.
4. Bedikian AY, Johnson MM, Warneke CL, Papadopoulos NE, Kim K, et al. (2008) Prognostic factors that determine the long-term survival of patients with unresectable metastatic melanoma. *Cancer Invest* 26: 624-633.
5. Korn EL, Liu PY, Lee SJ, Chapman JA, Niedzwiecki D, et al. (2008) Metaanalysis of phase II cooperative group trials in metastatic stage IV

- melanoma to determine progression-free and overall survival benchmarks for future phase II trials. *J Clin Oncol* 26: 527-534.
6. Balch CM, Gershenwald JE, Soong SJ, Thompson JF, Atkins MB, et al. (2009) Final version of 2009 AJCC melanoma staging and classification. *J Clin Oncol* 27: 6199-6206.
 7. Tsao H, Atkins MB, Sober AJ (2004) Management of cutaneous melanoma. *N Engl J Med* 351: 998-1012.
 8. Ives NJ, Stowe RL, Lorigan P, Wheatley K (2007) Chemotherapy compared with biochemotherapy for the treatment of metastatic melanoma: a meta-analysis of 18 trials involving 2,621 patients. *J Clin Oncol* 25: 5426-5434.
 9. Rudolf K, Cervinka M, Rudolf E (2009) Cytotoxicity and mitochondrial apoptosis induced by etoposide in melanoma cells. *Cancer Invest* 27: 704-717.
 10. Prausnitz MR, Langer R (2008) Transdermal drug delivery. *Nat Biotechnol* 26: 1261-1268.
 11. Swain S, Beg S, Singh A, Patro ChN, Rao ME (2011) Advanced techniques for penetration enhancement in transdermal drug delivery system. *Curr Drug Deliv* 8: 456-73.
 12. Guy RH, Hadgraft J (2009) Transdermal drug delivery. *Nat Biotechnol* 26: 1261-1268.
 13. Williams A (2004) Transdermal and topical drug delivery (1st edn.). Pharmaceutical Press, London.
 14. Prausnitz MR, Mitragotri S, Langer R (2004) Current status and future potential of transdermal drug delivery. *Nat Rev Drug Discov* 3: 115-124.
 15. Kumar A, Chen F, Mozhi A, Zhang X, Zhao Y, et al. (2013) Innovative pharmaceutical development based on unique properties of nanoscale delivery formulation. *Nanoscale* 5: 8307-8325.
 16. Bronaugh RL, Maibach HI (2005) Percutaneous absorption: drugs, cosmetics, mechanisms, methods (4th edn.). CRC Press, Boca Raton, FL.
 17. Shashank A, Shehata M, Morris DL, Thompson JF (2014) Radiofrequency ablation in metastatic melanoma. *J Surg Oncol* 109: 366-369.
 18. D'Agostino LG, Salomão Junior A, Viana DC, et al. (2014) The histological analysis by transdermal drug delivery on melanoma therapy. In: Méndez-Vilas A (ed), *Microscopy: advances in scientific research and education* (6th edn.). Formatex, Badajoz, pp. 348-355.
 19. Rastogi V, Pragya, Upadhyay P (2012) Brief view on antihypertensive drugs through transdermal patches. *Indian J Med Res Pharm Sci* 3: 1955-1970.
 20. Jamakandi VG, Mulla JS, Vinay BL, Shivakumar HN (2009) Formulation, characterization, and evaluation of matrix-type transdermal patches of a model antihypertensive drug. *Asian J Pharm* 3: 59-65.
 21. Sadhana P, Gupta SP, Jain SK (2005) Effective and controlled transdermal delivery of metoprolol tartarate. *Indian J Pharm Sci* 67: 346-350.
 22. Shin SC, Cho CW (2004) Enhanced transdermal delivery of atenolol from the ethylene-vinyl acetate matrix. *Int J Pharm* 287: 67-71.
 23. Sachan S, Bajpai M (2013) Transdermal drug delivery system: a review. *Int J Res Dev Pharm L Sci* 3: 748-765.
 24. Kumar R, Philip A (2007) Modified transdermal technologies: breaking the barriers of drug permeation via the skin. *Trop J Pharm Res* 6: 633-644.
 25. Galit L (2008) Advances in radio-frequency transdermal drug delivery.
 26. Sintov AC, Krymberk I, Daniel D, Hannan T, Sohn Z, et al. (2003) Radiofrequency microchanneling as a new way for electrically assisted transdermal delivery of hydrophilic drugs. *J Control Release* 89: 311-320.
 27. Nelson DA, Curran AR, Nyberg HA, Marttila EA, Mason PA, et al. (2013) High-resolution simulations of the thermophysiological effects of human exposure to 100 MHz RF energy. *Phys Med Biol* 58: 1947-1968.
 28. Beltrán-Frutos E, Bernal-Mañas CM, Navarro S, Zuasti A, Ferrer C, et al. (2012) Histological changes in connective tissue of rat tails after bipolar radiofrequency treatment. *Histol Histopathol* 7: 1231-1237.
 29. Xin F, Li-hong L, Alexiades-Armenakas M, Lueberding S, Cui-ping S, et al. (2013) Histological and electron microscopic analysis of fractional micro-plasma radio-frequency technology effects. *J Drugs Dermatol* 2: 1210-1214.
 30. Otake Y, Mims A, Fernandes DJ (2006) Merbarone induces activation of caspase-activated DNase and excision of chromosomal DNA loops from the nuclear matrix. *Mol Pharmacol* 69: 1477-1485.